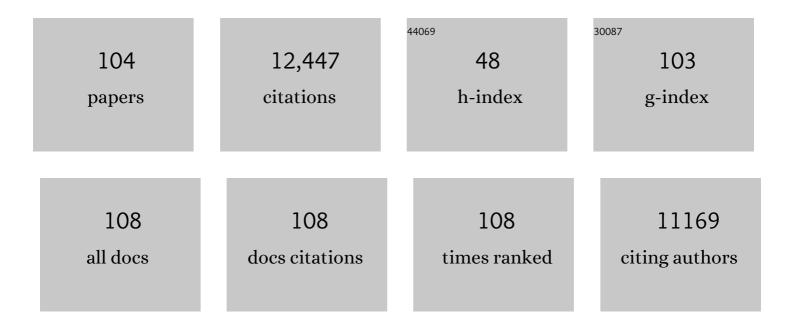
List of Publications by Year in descending order

Source: https://exaly.com/author-pdf/8470997/publications.pdf Version: 2024-02-01



Χιλογλη Γιμ

#	Article	IF	CITATIONS
1	FeOx-supported platinum single-atom and pseudo-single-atom catalysts for chemoselective hydrogenation of functionalized nitroarenes. Nature Communications, 2014, 5, 5634.	12.8	890
2	Remarkable Performance of Ir <sub>1</sub> /FeO <sub><i>x</i></sub> Single-Atom Catalyst in Water Gas Shift Reaction. Journal of the American Chemical Society, 2013, 135, 15314-15317.	13.7	811
3	Discriminating Catalytically Active FeN <sub><i>x</i></sub> Species of Atomically Dispersed Fe–N–C Catalyst for Selective Oxidation of the C–H Bond. Journal of the American Chemical Society, 2017, 139, 10790-10798.	13.7	738
4	Single-atom dispersed Co–N–C catalyst: structure identification and performance for hydrogenative coupling of nitroarenes. Chemical Science, 2016, 7, 5758-5764.	7.4	571
5	Ag Alloyed Pd Single-Atom Catalysts for Efficient Selective Hydrogenation of Acetylene to Ethylene in Excess Ethylene. ACS Catalysis, 2015, 5, 3717-3725.	11.2	545
6	Strong Metal–Support Interactions between Gold Nanoparticles and ZnO Nanorods in CO Oxidation. Journal of the American Chemical Society, 2012, 134, 10251-10258.	13.7	518
7	Non defect-stabilized thermally stable single-atom catalyst. Nature Communications, 2019, 10, 234.	12.8	452
8	Highly Efficient Catalysis of Preferential Oxidation of CO in H <sub>2</sub> -Rich Stream by Gold Single-Atom Catalysts. ACS Catalysis, 2015, 5, 6249-6254.	11.2	380
9	Performance of Cu-Alloyed Pd Single-Atom Catalyst for Semihydrogenation of Acetylene under Simulated Front-End Conditions. ACS Catalysis, 2017, 7, 1491-1500.	11.2	374
10	PdZn Intermetallic Nanostructure with Pd–Zn–Pd Ensembles for Highly Active and Chemoselective Semi-Hydrogenation of Acetylene. ACS Catalysis, 2016, 6, 1054-1061.	11.2	334
11	Strong Metal–Support Interactions between Pt Single Atoms and TiO <sub>2</sub> . Angewandte Chemie - International Edition, 2020, 59, 11824-11829.	13.8	309
12	Au–Cu Alloy nanoparticles confined in SBA-15 as a highly efficient catalyst for CO oxidation. Chemical Communications, 2008, , 3187.	4.1	288
13	Unraveling the coordination structure-performance relationship in Pt1/Fe2O3 single-atom catalyst. Nature Communications, 2019, 10, 4500.	12.8	279
14	Synthesis of Thermally Stable and Highly Active Bimetallic Auâ^'Ag Nanoparticles on Inert Supports. Chemistry of Materials, 2009, 21, 410-418.	6.7	262
15	Structural changes of Au–Cu bimetallic catalysts in CO oxidation: In situ XRD, EPR, XANES, and FT-IR characterizations. Journal of Catalysis, 2011, 278, 288-296.	6.2	260
16	Co–N–C Catalyst for C–C Coupling Reactions: On the Catalytic Performance and Active Sites. ACS Catalysis, 2015, 5, 6563-6572.	11.2	260
17	A Durable Nickel Singleâ€Atom Catalyst for Hydrogenation Reactions and Cellulose Valorization under Harsh Conditions. Angewandte Chemie - International Edition, 2018, 57, 7071-7075.	13.8	243
18	Efficient and Durable Au Alloyed Pd Single-Atom Catalyst for the Ullmann Reaction of Aryl Chlorides in Water. ACS Catalysis, 2014, 4, 1546-1553.	11.2	221

#	Article	IF	CITATIONS
19	Dynamic Behavior of Single-Atom Catalysts in Electrocatalysis: Identification of Cu-N <sub>3</sub> as an Active Site for the Oxygen Reduction Reaction. Journal of the American Chemical Society, 2021, 143, 14530-14539.	13.7	218
20	Strong metal-support interaction promoted scalable production of thermally stable single-atom catalysts. Nature Communications, 2020, 11, 1263.	12.8	198
21	Potential-Driven Restructuring of Cu Single Atoms to Nanoparticles for Boosting the Electrochemical Reduction of Nitrate to Ammonia. Journal of the American Chemical Society, 2022, 144, 12062-12071.	13.7	192
22	lridium Single-Atom Catalyst Performing a Quasi-homogeneous Hydrogenation Transformation of CO2 to Formate. CheM, 2019, 5, 693-705.	11.7	181
23	Understanding the synergistic effects of gold bimetallic catalysts. Journal of Catalysis, 2013, 308, 258-271.	6.2	178
24	Highly Selective Hydrogenation of CO <sub>2</sub> to Ethanol via Designed Bifunctional Ir <sub>1</sub> –In <sub>2</sub> O <sub>3</sub> Single-Atom Catalyst. Journal of the American Chemical Society, 2020, 142, 19001-19005.	13.7	158
25	Acid-Promoter-Free Ethylene Methoxycarbonylation over Ru-Clusters/Ceria: The Catalysis of Interfacial Lewis Acid–Base Pair. Journal of the American Chemical Society, 2018, 140, 4172-4181.	13.7	157
26	Influence of pretreatment temperature on catalytic performance of rutile TiO2-supported ruthenium catalyst in CO2 methanation. Journal of Catalysis, 2016, 333, 227-237.	6.2	154
27	Highly selective and robust single-atom catalyst Ru1/NC for reductive amination of aldehydes/ketones. Nature Communications, 2021, 12, 3295.	12.8	152
28	Promotional effect of Pd single atoms on Au nanoparticles supported on silica for the selective hydrogenation of acetylene in excess ethylene. New Journal of Chemistry, 2014, 38, 2043.	2.8	151
29	ZnAlâ€Hydrotalcite‣upported Au <sub>25</sub> Nanoclusters as Precatalysts for Chemoselective Hydrogenation of 3â€Nitrostyrene. Angewandte Chemie - International Edition, 2017, 56, 2709-2713.	13.8	127
30	Structural and catalytic properties of supported Ni–Ir alloy catalysts for H2 generation via hydrous hydrazine decomposition. Applied Catalysis B: Environmental, 2014, 147, 779-788.	20.2	116
31	Aerobic oxidative coupling of alcohols and amines over Au–Pd/resin in water: Au/Pd molar ratios switch the reaction pathways to amides or imines. Green Chemistry, 2013, 15, 2680.	9.0	114
32	Controlling CO <sub>2</sub> Hydrogenation Selectivity by Metal‣upported Electron Transfer. Angewandte Chemie - International Edition, 2020, 59, 19983-19989.	13.8	114
33	Acetylene-Selective Hydrogenation Catalyzed by Cationic Nickel Confined in Zeolite. Journal of the American Chemical Society, 2019, 141, 9920-9927.	13.7	112
34	Theoretical Insights and the Corresponding Construction of Supported Metal Catalysts for Highly Selective CO <sub>2</sub> to CO Conversion. ACS Catalysis, 2017, 7, 4613-4620.	11.2	104
35	Remarkable effect of alkalis on the chemoselective hydrogenation of functionalized nitroarenes over high-loading Pt/FeO <sub>x</sub> catalysts. Chemical Science, 2017, 8, 5126-5131.	7.4	90
36	Synergy of the catalytic activation on Ni and the CeO <sub>2</sub> –TiO <sub>2</sub> /Ce <sub>2</sub> Ti <sub>2</sub> O <sub>7</sub> stoichiometric redox cycle for dramatically enhanced solar fuel production. Energy and Environmental Science, 2019, 12, 767-779.	30.8	90

#	Article	IF	CITATIONS
37	Ru/TiO <sub>2</sub> Catalysts with Size-Dependent Metal/Support Interaction for Tunable Reactivity in Fischer–Tropsch Synthesis. ACS Catalysis, 2020, 10, 12967-12975.	11.2	83
38	Phosphorus coordinated Rh single-atom sites on nanodiamond as highly regioselective catalyst for hydroformylation of olefins. Nature Communications, 2021, 12, 4698.	12.8	78
39	Crystal phase effects on the structure and performance of ruthenium nanoparticles for CO <sub>2</sub> hydrogenation. Catalysis Science and Technology, 2014, 4, 2058-2063.	4.1	77
40	Photo–thermo Catalytic Oxidation over a TiO <sub>2</sub> â€WO <sub>3</sub> ‣upported Platinum Catalyst. Angewandte Chemie - International Edition, 2020, 59, 12909-12916.	13.8	75
41	Corking and Uncorking a Catalytic Yolk-Shell Nanoreactor: Stable Gold Catalyst in Hollow Silica Nanosphere. Journal of Physical Chemistry Letters, 2011, 2, 2984-2988.	4.6	72
42	High-Efficiency Water Gas Shift Reaction Catalysis on α-MoC Promoted by Single-Atom Ir Species. ACS Catalysis, 2021, 11, 5942-5950.	11.2	65
43	A Durable Nickel Singleâ€Atom Catalyst for Hydrogenation Reactions and Cellulose Valorization under Harsh Conditions. Angewandte Chemie, 2018, 130, 7189-7193.	2.0	64
44	Hierarchical Echinus-like Cu-MFI Catalysts for Ethanol Dehydrogenation. ACS Catalysis, 2020, 10, 13624-13629.	11.2	63
45	Cleavage of lignin C–O bonds over a heterogeneous rhenium catalyst through hydrogen transfer reactions. Green Chemistry, 2019, 21, 5556-5564.	9.0	62
46	Engineering of Yolk/Core–Shell Structured Nanoreactors for Thermal Hydrogenations. Small, 2021, 17, e1906250.	10.0	60
47	Defect-Mediated Gold Substitution Doping in ZnO Mesocrystals and Catalysis in CO Oxidation. ACS Catalysis, 2016, 6, 115-122.	11.2	54
48	Tuning the coordination environment of single-atom catalyst M-N-C towards selective hydrogenation of functionalized nitroarenes. Nano Research, 2022, 15, 519-527.	10.4	53
49	Nonprecious bimetallic Fe, Mo-embedded N-enriched porous biochar for efficient oxidation of aqueous organic contaminants. Journal of Hazardous Materials, 2022, 422, 126776.	12.4	53
50	Strong Metal–Support Interaction of Ru on TiO <sub>2</sub> Derived from the Co-Reduction Mechanism of Ru <sub><i>x</i></sub> Ti <sub>1–<i>x</i></sub> O <sub>2</sub> Interphase. ACS Catalysis, 2022, 12, 1697-1705.	11.2	49
51	Strong Metal–Support Interactions between Pt Single Atoms and TiO <sub>2</sub> . Angewandte Chemie, 2020, 132, 11922-11927.	2.0	46
52	RuO <sub>2</sub> /rutile-TiO <sub>2</sub> : a superior catalyst for N <sub>2</sub> O decomposition. Journal of Materials Chemistry A, 2014, 2, 5178-5181.	10.3	45
53	Selective hydrogenation of acetylene in an ethylene-rich stream over silica supported Ag-Ni bimetallic catalysts. Applied Catalysis A: General, 2017, 545, 90-96.	4.3	45
54	Isolation of Pd atoms by Cu for semi-hydrogenation of acetylene: Effects of Cu loading. Chinese Journal of Catalysis, 2017, 38, 1540-1548.	14.0	44

#	Article	IF	CITATIONS
55	Sustainable Carbon Materials toward Emerging Applications. Small Methods, 2021, 5, e2001250.	8.6	44
56	Crystal-Phase-Mediated Restructuring of Pt on TiO <sub>2</sub> with Tunable Reactivity: Redispersion versus Reshaping. ACS Catalysis, 2022, 12, 3634-3643.	11.2	44
57	SiO 2 -supported Au-Ni bimetallic catalyst for the selective hydrogenation of acetylene. Chinese Journal of Catalysis, 2017, 38, 1338-1346.	14.0	42
58	Metabolomic profiling of emodin-induced cytotoxicity in human liver cells and mechanistic study. Toxicology Research, 2015, 4, 948-955.	2.1	40
59	ZnAlâ€Hydrotalciteâ€6upported Au <sub>25</sub> Nanoclusters as Precatalysts for Chemoselective Hydrogenation of 3â€Nitrostyrene. Angewandte Chemie, 2017, 129, 2753-2757.	2.0	40
60	Effects of divalent metal ions of hydrotalcites on catalytic behavior of supported gold nanocatalysts for chemoselective hydrogenation of 3-nitrostyrene. Journal of Catalysis, 2018, 364, 174-182.	6.2	35
61	Amorphous Cobalt Oxide Nanoparticles as Active Waterâ€Oxidation Catalysts. ChemCatChem, 2017, 9, 3641-3645.	3.7	34
62	A novel CeO <sub>2</sub> – <i>x</i> SnO <sub>2</sub> /Ce <sub>2</sub> Sn <sub>2</sub> O <sub>7</sub> pyrochlore cycle for enhanced solar thermochemical water splitting. AICHE Journal, 2017, 63, 3450-3462.	3.6	34
63	Dual-Functional Titanium(IV) Immobilized Metal Affinity Chromatography Approach for Enabling Large-Scale Profiling of Protein Mannose-6-Phosphate Glycosylation and Revealing Its Predominant Substrates. Analytical Chemistry, 2019, 91, 11589-11597.	6.5	34
64	Synthesis and characterization of iron-nitrogen-doped biochar catalysts for organic pollutant removal and hexavalent chromium reduction. Journal of Colloid and Interface Science, 2022, 610, 334-346.	9.4	34
65	Immobilized Ni Clusters in Mesoporous Aluminum Silica Nanospheres for Catalytic Hydrogenolysis of Lignin. ACS Sustainable Chemistry and Engineering, 2019, 7, 19034-19041.	6.7	32
66	Dual-Functional Ti(IV)-IMAC Material Enables Simultaneous Enrichment and Separation of Diverse Glycopeptides and Phosphopeptides. Analytical Chemistry, 2021, 93, 8568-8576.	6.5	32
67	High-loading and thermally stable Pt1/MgAl1.2Fe0.8O4 single-atom catalysts for high-temperature applications. Science China Materials, 2020, 63, 949-958.	6.3	31
68	A Novel Singleâ€Atom Electrocatalyst Ti <sub>1</sub> /rGO for Efficient Cathodic Reduction in Hybrid Photovoltaics. Advanced Materials, 2020, 32, e2000478.	21.0	31
69	Near 100% ethene selectivity achieved by tailoring dual active sites to isolate dehydrogenation and oxidation. Nature Communications, 2021, 12, 5447.	12.8	30
70	Synthesis of bio-based methylcyclopentadiene via direct hydrodeoxygenation of 3-methylcyclopent-2-enone derived from cellulose. Nature Communications, 2021, 12, 46.	12.8	27
71	Sulfate-Modified NiAl Mixed Oxides as Effective C–H Bond-Breaking Agents for the Sole Production of Ethylene from Ethane. ACS Catalysis, 2020, 10, 7619-7629.	11.2	26
72	Atomic Pyridinic Nitrogen Sites Promoting Levulinic Acid Hydrogenations over Double‣helled Hollow Ru/C Nanoreactors. Small, 2021, 17, e2101271.	10.0	26

#	Article	IF	CITATIONS
73	Selective Hydrogenation of Acetylene over SBAâ€15 Supported Au—Cu Bimetallic Catalysts. Journal of the Chinese Chemical Society, 2013, 60, 907-914.	1.4	24
74	Producing of cinnamyl alcohol from cinnamaldehyde over supported gold nanocatalyst. Chinese Journal of Catalysis, 2021, 42, 470-481.	14.0	23
75	Crystallinity-Modulated Co <sub>2–<i>x</i></sub> V <sub><i>x</i></sub> O <sub>4</sub> Nanoplates for Efficient Electrochemical Water Oxidation. ACS Catalysis, 2021, 11, 14884-14891.	11.2	23
76	Introducing Co–O Moiety to Co–N–C Single-Atom Catalyst for Ethylbenzene Dehydrogenation. ACS Catalysis, 2022, 12, 7760-7772.	11.2	23
77	Relation between Water Oxidation Activity and Coordination Environment of C,N-Coordinated Mononuclear Co Catalyst. ACS Catalysis, 2022, 12, 491-496.	11.2	22
78	Metabolomic Responses of Human Hepatocytes to Emodin, Aristolochic Acid, and Triptolide: Chemicals Purified from Traditional Chinese Medicines. Journal of Biochemical and Molecular Toxicology, 2015, 29, 533-543.	3.0	21
79	A metabolomics study of the inhibitory effect of 17-beta-estradiol on osteoclast proliferation and differentiation. Molecular BioSystems, 2015, 11, 635-646.	2.9	20
80	One-Step SH2 Superbinder-Based Approach for Sensitive Analysis of Tyrosine Phosphoproteome. Journal of Proteome Research, 2019, 18, 1870-1879.	3.7	18
81	Effect of IB-metal on Ni/SiO2 catalyst for selective hydrogenation of acetylene. Chinese Journal of Catalysis, 2020, 41, 1099-1108.	14.0	18
82	Selective catalytic oxidation of ammonia to nitric oxide via chemical looping. Nature Communications, 2022, 13, 718.	12.8	18
83	Rapid and sensitive analysis of parishin and its metabolites in rat plasma using ultra high performance liquid chromatography-fluorescence detection. Journal of Chromatography B: Analytical Technologies in the Biomedical and Life Sciences, 2014, 973, 104-109.	2.3	17
84	Crystal Plane Effect of ZnO on the Catalytic Activity of Gold Nanoparticles for the Acetylene Hydrogenation Reaction. Journal of Physical Chemistry C, 2017, 121, 19727-19734.	3.1	17
85	Photo–thermo Catalytic Oxidation over a TiO 2 â€₩O 3 ‣upported Platinum Catalyst. Angewandte Chemie, 2020, 132, 13009-13016.	2.0	15
86	Identification of Angiotensin l onverting Enzyme Inhibitors in Peptides Mixture of Hydrolyzed Red Deer Plasma with Proteomic Approach. Chinese Journal of Chemistry, 2010, 28, 1665-1672.	4.9	13
87	Effective removal of the protective ligands from Au nanoclusters by ambient pressure nonthermal plasma treatment for CO oxidation. Chinese Journal of Catalysis, 2018, 39, 929-936.	14.0	13
88	Detecting Proteins Glycosylation by a Homogeneous Reaction System with Zwitterionic Gold Nanoclusters. Analytical Chemistry, 2017, 89, 4339-4343.	6.5	12
89	Highly Efficient Enrichment of O-GalNAc Clycopeptides by Using Immobilized Metal Ion Affinity Chromatography. Analytical Chemistry, 2021, 93, 7579-7587.	6.5	12
90	Active and stable Cu doped NiMgAlO catalysts for upgrading ethanol to n-butanol. Journal of Energy Chemistry, 2022, 72, 306-317.	12.9	12

#	Article	IF	CITATIONS
91	Metal-Support Synergy of Supported Gold Nanoclusters in Selective Oxidation of Alcohols. Catalysts, 2020, 10, 107.	3.5	11
92	Synthesis of Subnanometer‣ized Gold Clusters by a Simple Millingâ€Mediated Solid Reduction Method. Chinese Journal of Chemistry, 2018, 36, 329-332.	4.9	10
93	Design of an Amphiphilic Perylene Diimide for Optical Recognition of Anticancer Drug through a Chiralityâ€Induced Helical Structure. Chemistry - A European Journal, 2019, 25, 9834-9839.	3.3	10
94	Water-soluble Au nanoclusters for multiplexed mass spectrometry imaging. Chemical Communications, 2017, 53, 12688-12691.	4.1	9
95	Controlling CO 2 Hydrogenation Selectivity by Metalâ€Supported Electron Transfer. Angewandte Chemie, 2020, 132, 20158-20164.	2.0	8
96	Acute nephrotoxicity of aristolochic acidin vitro: metabolomics study for intracellular metabolic time-course changes. Biomarkers, 2016, 21, 233-242.	1.9	6
97	Study of Surface Plasmon Assisted Reactions to Understand the Light-Induced Decarboxylation of N719 Sensitizer. European Journal of Inorganic Chemistry, 2019, 2019, 23-28.	2.0	6
98	Oxidative coupling of methane over Mo–Sn catalysts. Chemical Communications, 2021, 57, 13297-13300.	4.1	4
99	A Tyrosine Phosphoproteome Analysis Approach Enabled by Selective Dephosphorylation with Protein Tyrosine Phosphatase. Analytical Chemistry, 2022, 94, 4155-4164.	6.5	4
100	Submicroreactors: Enhanced Hydrogenation Performance over Hollow Structured Co oO <i>x</i> @N  Capsules (Adv. Sci. 22/2019). Advanced Science, 2019, 6, 1970135.	11.2	3
101	A New Workflow for the Analysis of Phosphosite Occupancy in Paired Samples by Integration of Proteomics and Phosphoproteomics Data Sets. Journal of Proteome Research, 2020, 19, 3807-3816.	3.7	3
102	Constructing the Supporting Service, Education Guidance, Management System of Network Education and Examination. , 2013, , .		2
103	Chemoselective hydrogenation of 3â€nitrostyrene over supported gold catalysts: Effect of loadings of gold. Journal of the Chinese Chemical Society, 2021, 68, 444-450.	1.4	2
104	Comprehensive chemical profile and quantitative analysis of the Shabyar tablet, a traditional ethnic medicine prescription, by ultraâ€highâ€performance liquid chromatography with quadrupoleâ€orbitrap highâ€resolution mass spectrometry. Journal of Separation Science, 2022, 45, 2148-2160.	2.5	2